

AD-A051 719

COLORADO UNIV DENVER MEDICAL CENTER

F/G 6/16

PULMONARY GAS TRANSPORT AND THE REGULATION OF VENTILATION AT RE--ETC(U)

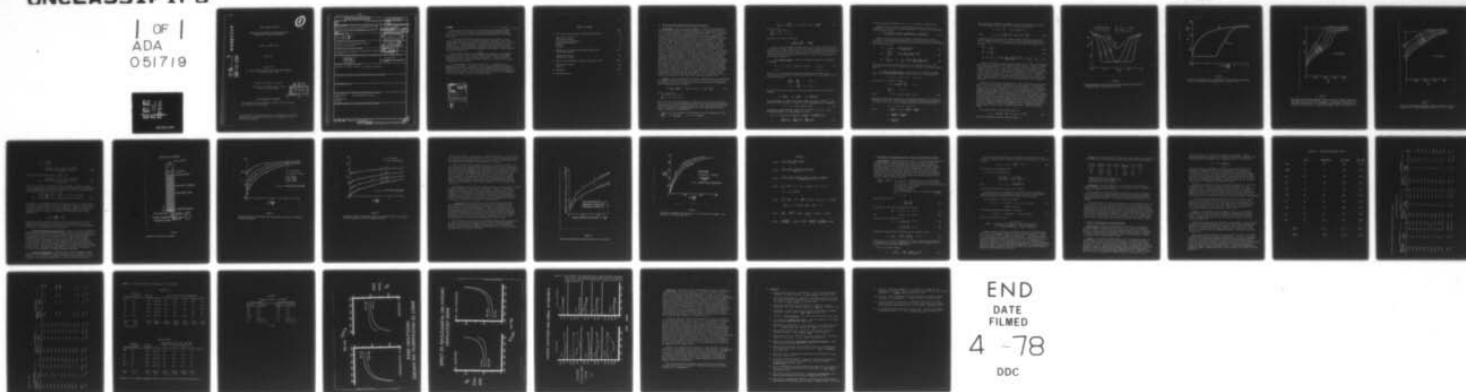
APR 74 G F FILLEY

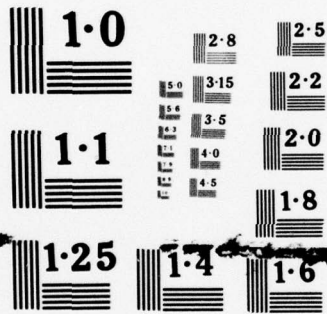
DADA17-72-C-2090

NL

UNCLASSIFIED

1 OF 1
ADA
051719





NATIONAL BUREAU OF STANDARDS
MICROCOPY RESOLUTION TEST CHART

AD A 051719

AD NO. _____
DDC FILE COPY

①
52

FINAL PROGRESS REPORT

PULMONARY GAS TRANSPORT AND THE REGULATION OF
VENTILATION AT REST AND EXERCISE

GILES F. FILLEY, M.D.

APRIL 1974

Supported By

U.S. ARMY MEDICAL RESEARCH AND DEVELOPMENT COMMAND
Washington, D.C. 20314

Contract No. DADA 17-72-C-2090

University of Colorado Medical Center
Denver, Colorado 80220

DDC
RECEIVED
MAR 22 1978
D

DDC AVAILABILITY STATEMENT

This document has been approved for public release and sale;
its distribution is unlimited.

The findings in this report are not to be construed as an official
Department of the Army position unless so designated by other
authorized documents.

REPORT DOCUMENTATION PAGE		READ INSTRUCTIONS BEFORE COMPLETING FORM
1. REPORT NUMBER 6	2. GOVT ACCESSION NO.	3. RECIPIENT'S CATALOG NUMBER 9
4. TITLE (and Subtitle) Pulmonary Gas Transport and the Regulation of Ventilation at Rest and Exercise		5. TYPE OF REPORT & PERIOD COVERED Final Report 1 Jan 1972 - 30 June 1972
6. AUTHOR(s) Giles F. Filley M. D.		7. PERFORMING ORG. REPORT NUMBER
9. PERFORMING ORGANIZATION NAME AND ADDRESS University of Colorado Medical Center Denver, Colorado 80220		8. CONTRACT OR GRANT NUMBER(s) 15 DADA 17-72-C-2090 ^{ew}
11. CONTROLLING OFFICE NAME AND ADDRESS US Army Medical Research and Development Command Washington, D. C. 20314		10. PROGRAM ELEMENT, PROJECT, TASK AREA & WORK UNIT NUMBERS 62110A 16 3A162110A82700.034
14. MONITORING AGENCY NAME & ADDRESS (if different from Controlling Office) 12/34p.		12. REPORT DATE 11 Apr 1974
		13. NUMBER OF PAGES 35 pages
		15. SECURITY CLASS. (of this report) Unclassified
		15a. DECLASSIFICATION/DOWNGRADING SCHEDULE
16. DISTRIBUTION STATEMENT (of this Report) Approved for public release; distribution unlimited		
17. DISTRIBUTION STATEMENT (of the abstract entered in Block 20, if different from Report)		
18. SUPPLEMENTARY NOTES		
19. KEY WORDS (Continue on reverse side if necessary and identify by block number) Oxygen uptake blood oxygenation analysis Blood Pentobarbital Hypoxia		
20. ABSTRACT (Continue on reverse side if necessary and identify by block number)		

AB

SUMMARY

During this report period work concentrated

During the last six months of this contract the emphasis has been on the completion of studies in progress for which continued support would not be available. The work has been concentrated in the following three areas:

on the following topics:

(1) A theoretical and experimental study of the O₂ uptake by blood in the human lung and in the artificial membrane oxygenator. The rate of oxygen uptake by blood under various conditions is of physiological interest as well as of clinical importance. This work includes a study of blood oxygenation in a tubular membrane oxygenator under controlled conditions with the purpose of determining the parameters governing the oxygen transport under these conditions.

(2) An improved method for measuring the CO diffusing capacity (D_{CO}) has been developed. Earlier methods had the shortcomings of requiring end-tidal gas samples or an arterial blood sample. A new steady state method which does not require end-tidal sampling or invasion of the subject is described in this report

(3) Pentobarbital is a commonly used drug as a premedication for anesthesia and surgery. Hypoxia is always a danger during anesthesia and an investigation of the depression of the ventilatory drive mechanisms is described in this report. It is anticipated that this work will better allow clinicians to predict the patients in whom administration of this drug would result in depression of hypoxic ventilatory drive.

ACCESSION BY	
NTIS	White Section <input checked="" type="checkbox"/>
DDC	Ref Section <input type="checkbox"/>
UNANNOUNCED	<input type="checkbox"/>
JUSTIFICATION	
BY	
DISTRIBUTION/AVAILABILITY CODES	
Dist.	AVAIL. and/or SPECIAL
A	

TABLE OF CONTENTS

	page
A. The O ₂ Diffusing Capacity of Blood at Two O ₂ Levels	1-16
Theoretical Analysis	1
The entrance region	2
The fully developed region	3
Experimental procedure	9
Results	9
Appendix	16
B. Measurement of CO Diffusion Capacity Using a New Steady State Method	17-19
Theoretical analysis	17
Experimental results	19
C. Effect of Pentobarbital on Hypoxic Ventilatory Drive	19-28
Experimental methods	19
Results	20
D. References	29-30
E. Distribution List	31

A. The O₂ Diffusing Capacity of Blood at Two O₂ Levels

Introduction: The rate of oxygen uptake by blood in the human lung as well as in the artificial membrane oxygenator is of physiological interest and of clinical importance. Recently, considerable attention has been paid to the characterization of blood oxygenators (1,3,5,7,8). In the present work, the study of blood oxygenation in a tubular membrane oxygenator is undertaken at various controlled conditions. Since the diameter of the tube is much greater than the size of a red cell, it is reasonable to consider blood as a homogeneous fluid with uniformly distributed red cells acting as oxygen sinks. Flow is assumed to be laminar with parabolic velocity profile and the process to be diffusion limited with negligible wall resistance. The reaction of O₂ with Hb is considered to be instantaneous; the P_{O₂} is considered to be the same in the red cell as in the plasma. The problem is investigated both theoretically and experimentally. In the former part, an integral method (4) is introduced to handle the non-linear diffusion equation. The main advantage of the integral method is that it changes the governing diffusion equation from a partial differential equation into an ordinary differential equation. The concept of this method is to define a diffusion boundary layer, δ , which is analogous to the hydrodynamic boundary layer (6). It is assumed that beyond the position δ there is no mass transfer and equilibrium exists. By integrating the governing differential equation with respect to the space variable over this layer, a first order ordinary differential equation can be obtained and its solution is usually tractable. In the experimental part, testing is done on human blood at different oxygen levels while varying the rate at which blood was pumped through the system. By comparing the theoretical and experimental results, both the overall diffusivity, D , and the diffusion capacity, D_L , can be determined. The D_L values are compared with the results from different approaches (2).

Analysis: Fully developed reduced blood of uniform plasma O₂ concentration, C_0 , enters the membrane tubing at $Z = 0$ where the ambient O₂ pressure is kept at constant value P_s . The steady state diffusion of O₂ can be described by the following differential equation

$$D \left[\frac{1}{r} \frac{\partial}{\partial r} \left(r \frac{\partial C}{\partial r} \right) \right] = 2V_m (1 + F_1) \left[1 - \left(\frac{r}{R} \right)^2 \right] \frac{\partial C}{\partial Z} \quad (1)$$

with $C = C_0$ at $Z = 0$
 $C = C_s$ at $r = R, Z > 0$
 $\frac{\partial C}{\partial r} = 0$ at $r = 0, z > 0$,

where D is the overall diffusivity, C represents the plasma O₂ concentration with $C = \alpha P$, V_m is the laminar mean velocity, r and Z are the radial and axial coordinates F_1 represents a sink function from the combination of O₂ with Hb with a strength of $F_1 = T_1 (dS/dC)$, where T_1 is the oxygen capacity of the normal blood and S is the saturation.

Equation (1) can be written in dimensionless form by introducing $r^* = \frac{r}{R}$;
 $\epsilon = \frac{\pi D Z}{2Q}$; $C^* = \frac{C - C_0}{C_s - C_0}$; $y = 1 - r^*$ yielding

$$\frac{\partial}{\partial y} \left[(1 - y) \frac{\partial C^*}{\partial y} \right] = (1 + F) y(2 - y)(1 - y) \frac{\partial C^*}{\partial \xi} \quad (2)$$

with $C^* = 0$ at $\xi = 0$
 $C^* = 1$ at $y = 0, \xi > 0$
 $\frac{\partial C^*}{\partial y} = 0$ at $y = 1, \xi > 0$.

where \dot{Q} is the blood flow rate and

$$F = \frac{T_1}{(C_s - C_0)} \frac{dS}{dC^*} = T \frac{dS}{dC^*}.$$

In order to solve equation (2) the entire flow is divided into two regions one being the entrance region in which the diffusion boundary layer develops and reaches the center line of the tube. This is followed by a fully developed diffusion-flow region in which the concentration at the center of the tube changes at different stations along the tube. Solutions for each region have to be sought separately.

(A) Entrance region: Let the concentration profile be expressed by a polynomial

$$\begin{aligned} C^* &= 1 + a_1 \left(\frac{y}{\delta} \right) + a_2 \left(\frac{y}{\delta} \right)^2 + a_3 \left(\frac{y}{\delta} \right)^3 & 0 \leq y \leq \delta \\ C^* &= 0 & \delta < y < 1 \end{aligned} \quad (3)$$

where δ is the dimensionless diffusion boundary layer thickness. The coefficients $a_1, a_2,$ and a_3 are functions of ξ which can be determined from the following conditions

$$\begin{aligned} \frac{\partial^2 C^*}{\partial y^2} &= \frac{\partial C^*}{\partial y} & \text{at } \frac{y}{\delta} &= 0 \\ C^* &= 0, \frac{\partial C^*}{\partial y} = 0 & \text{at } \frac{y}{\delta} &= 1 \end{aligned}$$

the first of which is obtained by evaluating equation (2) at the tube wall, yielding

$$a_1 = \frac{-6}{4 + \delta} \quad a_2 = \frac{-3\delta}{4 + \delta} \quad a_3 = \frac{2(1 + \delta)}{4 + \delta}.$$

The only unknown is δ which can be solved from the integral procedure. The saturation curve S at $\text{pH} = 7.4$ and 37°C can be approximated by a polynomial

$$S = b_0 + b_1 C^* + b_2 C^{*2} + b_3 C^{*3} \quad (4)$$

Integrating equation (2) with respect to y and from $y = 0$ to $y = \delta$, and introducing equation (3) and equation (4) yields

$$\begin{aligned} 6\xi &= (1 + Tb_1) H_1(\delta) + Tb_2 H_2(\delta) + Tb_3 H_3(\delta) - \frac{(1 + Tb_1)}{70} H_4(\delta) \\ &\quad - \frac{Tb_2}{420} H_5(\delta) - \frac{Tb_3}{20020} H_6(\delta) - \frac{Tb_3}{5005} H_7(\delta) \end{aligned} \quad (5)$$

where the expression $H_i(\delta)$ for $i = 1, 2 \dots 7$ are given in Appendix A.

Equation (5) gives the relation between ξ and δ with b_1, b_2, b_3 as parameters. At the end of the entrance region $\xi = \xi_0$ where δ has its maximum value of unity, we have

$$\xi_0 = \frac{0.2920939 (1 + Tb_1) + 0.175892 Tb_2 + 0.118688 Tb_3}{6} \quad (6)$$

Based on equation (3) the mass transfer characteristics may now be evaluated. This requires consideration of three distinct kinds of averages: the mean value \bar{C}^* , bulk mean value C_b^* , and the average value of C^* in each tube, \bar{C}^* . These are given as

$$\bar{C}^* = \frac{1}{A} \int C^* dA = \frac{30\delta + 2\delta^2 - 3\delta^3}{10(4 + \delta)} \quad (7)$$

$$C_b^* = \frac{\int VC^* dA}{\int V dA} = \frac{5\delta^5 - 16\delta^4 - 28\delta^3 - 112\delta^2}{35(4 + \delta)} \quad (8)$$

$$\bar{C}^* = \frac{1}{\xi} \int_0^\xi \bar{C}^* d\xi = \bar{C}^* - \frac{1}{\xi} \int_0^\delta \xi \left[\frac{120 + 16\delta - 34\delta^2 - 6\delta^3}{10(4 + \delta)^2} \right] \quad (9)$$

where A is the cross-sectional area and V is the laminar velocity. The saturation at the exit of the oxygenator can be obtained by utilizing equation (4).

(B) Fully developed region: In this region the diffusion boundary layer loses its meaning and the concentration profile is chosen simply as

$$C^* = f_0 - f_1 y - f_2 y^2 - f_3 y^3 \quad 0 \leq y \leq 1.$$

By utilizing the boundary conditions

$$C^* = 1 \text{ and } \frac{\partial^2 C^*}{\partial y^2} = \frac{\partial C^*}{\partial y} \quad \text{at } y = 0$$

$$\frac{\partial C^*}{\partial y} = 0 \quad \text{at } y = 1$$

we have
$$C^* = 1 - f_1 \left[y + \frac{1}{2} y^2 - \frac{2}{3} y^3 \right]. \quad (10)$$

Equation (10) shows the similarity in concentration distribution at different sections along the tube in this region. Integrating equation (2) with respect to y from $y = 0$ to $y = 1$ and by introducing equations (4) and (10) yields

$$\xi = -A \ln f_1 + B f_1 - E f_1^2 + G$$

where

$$A = \frac{17}{140} (1 + Tb_1) + \frac{17 Tb_2}{70} + \frac{51 Tb_3}{140}$$

$$B = \frac{101 Tb_2}{720} + \frac{101 Tb_3}{240}$$

$$E = \frac{15997 Tb_3}{240240}.$$

The integration constant G is obtained by using the continuity of solution from the entrance region to the fully developed region, that is

$$f_1 = a_1 = -\frac{6}{5} \quad \text{at } \xi = \xi_0 \text{ and } \delta = 1$$

$$\text{yields } \xi - \xi_0 = -A \ln \frac{5f_1}{6} + B(f_1 - \frac{6}{5}) - E(f_1^2 - \frac{36}{25}) . \quad (11)$$

Equations (10) and (11) give the complete solution for this region where f_1 has its maximum value of $6/5$ at $\xi - \xi_0 = 0$ and it approaches to zero as $\xi - \xi_0 \rightarrow \infty$ or $C^* \rightarrow 1.0$. The corresponding expression for \bar{C}^* , \bar{C}_b^* , and \bar{C}^* are given as

$$\bar{C}^* = 1 - \frac{7}{20} f_1 \quad (12)$$

$$\bar{C}_b^* = 1 - \frac{17}{35} f_1 \quad (13)$$

$$\bar{C}^* = \bar{C}_b^* - \frac{1}{\xi} \left\{ \int_0^1 \xi \left[\frac{120 + 16\delta - 34\delta^2 - 6\delta^3}{10(4 + \delta)^2} \right] d\delta + \frac{7}{20} \int_{f_1}^{1.2} \xi df_1 \right\} . \quad (14)$$

Figure 1 presents the results from equations (3), (4), (5), (10), and (11) which shows the dependence of saturation on both r/R and ξ . When $\xi < 1.6868$ the concentration profile is not fully developed, which corresponds to the entrance region. For $\xi > 1.6868$ the concentration at the center of the tube starts to increase, which corresponds to the solution from the fully developed region. Figure 2 depicts the bulk mean saturation, \bar{S}_b , and the saturation at the center line of the tube $S_{r=0}$. The delay rising of $S_{r=0}$ is due to the finite interval required for O_2 to diffuse from the wall to the center of the tube. The dimensionless length ξ_0 for the entrance region is the measure of this delay.

Figures 3 and 4 show the predicted time course of blood P_{O_2} at two ambient oxygen levels. The pressure ratio P_b/P_s is plotted against the time ratio t/t_{98} , where t_{98} is the time taken for P_b to reach 98% P_s . It is clear that $t/t_{98} = \xi/\xi_{98}$ from the definition of ξ ; hence the dimensionless time required for P_b/P_s to reach 98% is equal to ξ_{98} . At the higher ambient O_2 level, a sharply increasing P_b/P_s is observed in the early part of the process, whereas P_b/P_s increases with a steadily decreasing slope at the lower ambient O_2 level. This effect depends on the range of the dissociation curve where the operation is taking place. At the higher ambient P_{O_2} , the plateau of the dissociation curve is reached early and the strength of the sink is much reduced. After the Hb is saturated, additional O_2 uptake will only contribute to raising the plasma P_{O_2} . However, at the lower ambient O_2 level, a large sink effect exists during the whole process and P_b/P_s then shows a steadily increasing trend.

The oxygen uptake in each membrane tubing is

$$V_{O_2} = \dot{Q} \left\{ T(\bar{S}_b - S_0) + 22.4 (C_s - C_0) \bar{C}_b^* \right\} \quad (15)$$

and the corresponding diffusing capacity becomes

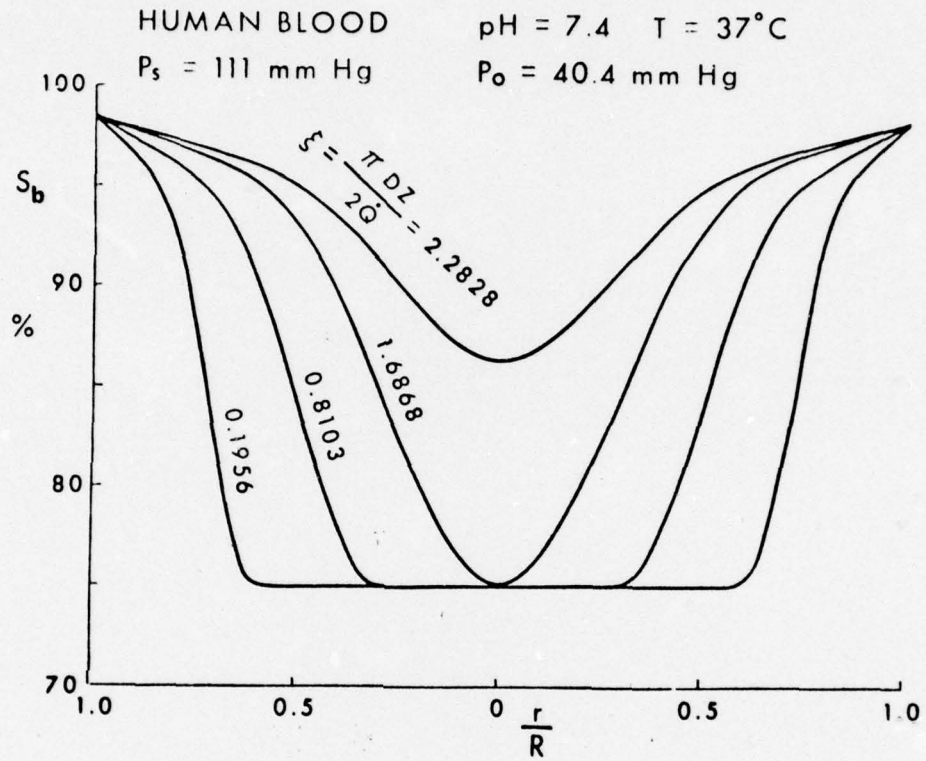


Figure 1

Oxygen saturations in the blood at various radial positions and at 4 (dimensionless) stations along the tube.

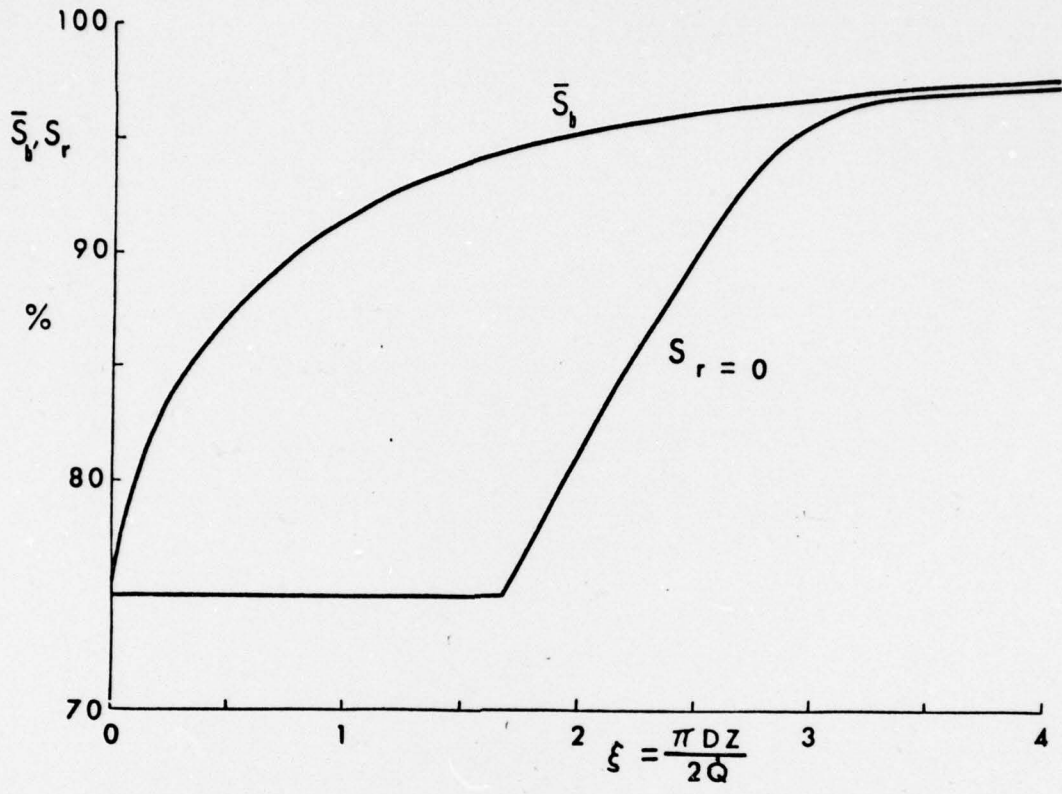


Figure 2

Bulk mean O_2 saturation and O_2 saturation at the center of the tubing for $P_s = 111$ mm Hg, $P_o = 40.4$ mm Hg, pH = 7.4 and $T = 37^\circ$ C.

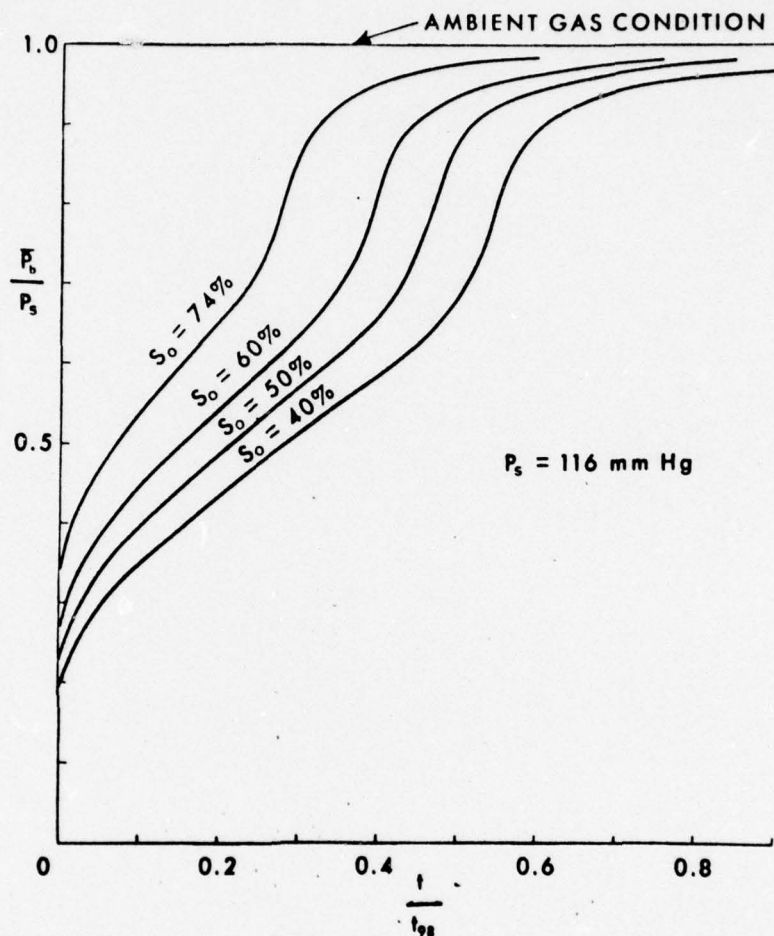


Figure 3

P_{O_2} time course along the membrane tubing at different initial saturations. The value of t_{98} is fixed in this figure; it is the time taken for P_0 to reach 98% of P_s when $S_0 = 40\%$. Holding it fixed provides a reference value so that the curves for $S_0 > 40\%$ can be compared. $\text{pH} = 7.4$, $T = 37^\circ \text{C}$.

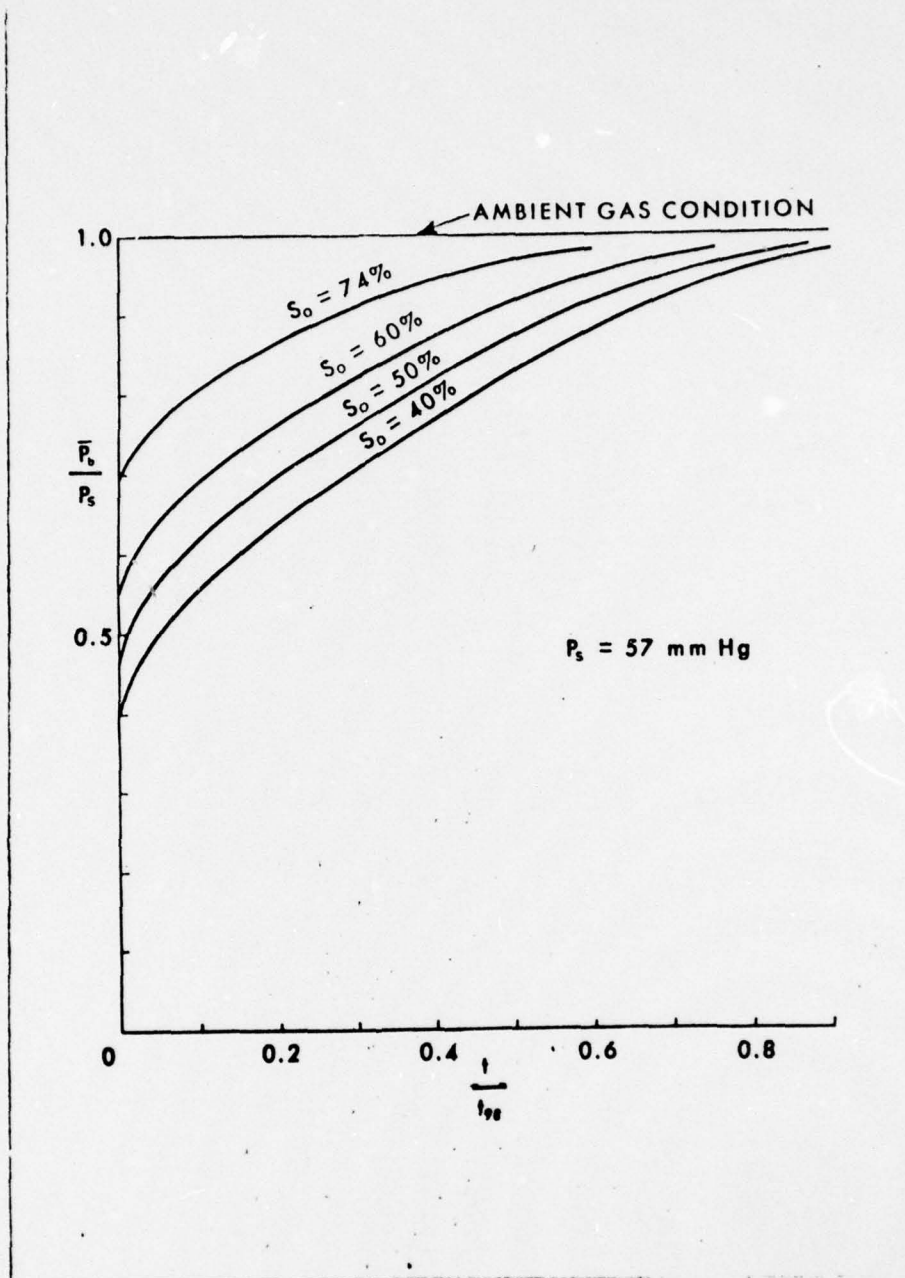


Figure 4

P_{O_2} time course along the membrane tubing at different initial saturations in a lower ambient O_2 level. $pH = 7.4$, $T = 37^\circ C$.

$$D_L = \frac{\dot{V}_{O_2}}{P_s - \bar{P}} = \frac{\dot{Q} \left\{ T (S_b - S_o) + 22.4 (C_s - C_o) \bar{C}_b^* \right\}}{P_s - \bar{P}} \quad (16a)$$

By utilizing the relation that $Q = \pi DZ/2\xi$, then

$$D_L = \frac{\pi DZ \left\{ T (\bar{S}_b - S_o) + 22.4 (C_s - C_o) \bar{C}_b^* \right\}}{2\xi (P_s - \bar{P})} \quad (16b)$$

At each value of ξ the appropriate values of \bar{S}_b , \bar{C}_b^* , and \bar{P} are all given. Z is the length of the tubing and D is determined by comparing the theoretical and experimental results. Equation (16a) can be written in a different form by introducing equation (4) into it, then

$$D_L = \frac{\dot{Q} \left\{ T \bar{C}_b^* \left(\frac{d\bar{S}_b}{d\bar{C}_b^*} - b_2 \bar{C}_b^* - 2b_3 \bar{C}_b^{*2} \right) + 22.4 (C_s - C_o) \bar{C}_b^* \right\}}{P_s - \bar{P}} \quad (16c)$$

In equation (16c), $d\bar{S}_b/d\bar{C}_b^*$ represents the strength of the sink effect, which is inversely proportional to the value of \bar{C}_b^* . The constant b_2 is the second derivative of the dissociation curve evaluated at the initial condition and is always a negative value. The quantity $(d\bar{S}_b/d\bar{C}_b^* - b_2 \bar{C}_b^*)$ is by far the dominant term in the numerator. Therefore the diffusing capacity can be expressed as

$$D_L \propto \dot{Q} \left[\frac{d\bar{S}_b}{d\bar{C}_b^*} - b_2 \bar{C}_b^* \right]$$

The above expression indicates that D_L is mainly proportional to the blood flow rate and the binding of O_2 in the red cells, which in turn, can be expressed as a function of the initial blood condition and the sink strength of the blood as it emerges from the oxygenator.

Experimental Apparatus and Procedure: Figure 5 shows the experimental apparatus which includes an oxygenator, a lucite isothermal testing chamber, a Harvard precision pump and a 10 cc syringe with water jacket for blood sample. The oxygenator consists of 12 identical Silastic Medical Grade membrane tubings (0.012 in I.D. x 0.025 in O.D. x 13.5 in long) with the entrance 1.4 inch coated by impermeable epoxy to guarantee the full development of velocity profile. The chamber is continuously flushed with a gas mixture of desired PO_2 and 4.5% of CO_2 to maintain constant pH. Heparinized fresh human blood at $37^\circ C$ is pumped through the oxygenator at steady rates from 4.12 cc/min to 0.103 cc/min. The oxygenated blood sample is collected and analyzed at the exit of the oxygenator by a SEGM pH- PO_2 - PCO_2 radiometer.

Results and Discussion: Figures 6 and 7 show the comparison between theoretical and experimental results. Each set of data is brought in close agreement with the analytical solution by finding a suitable value of D . The dependence of the bulk mean saturation \bar{S}_b on the initial saturation S_o is

TESTING CHAMBER

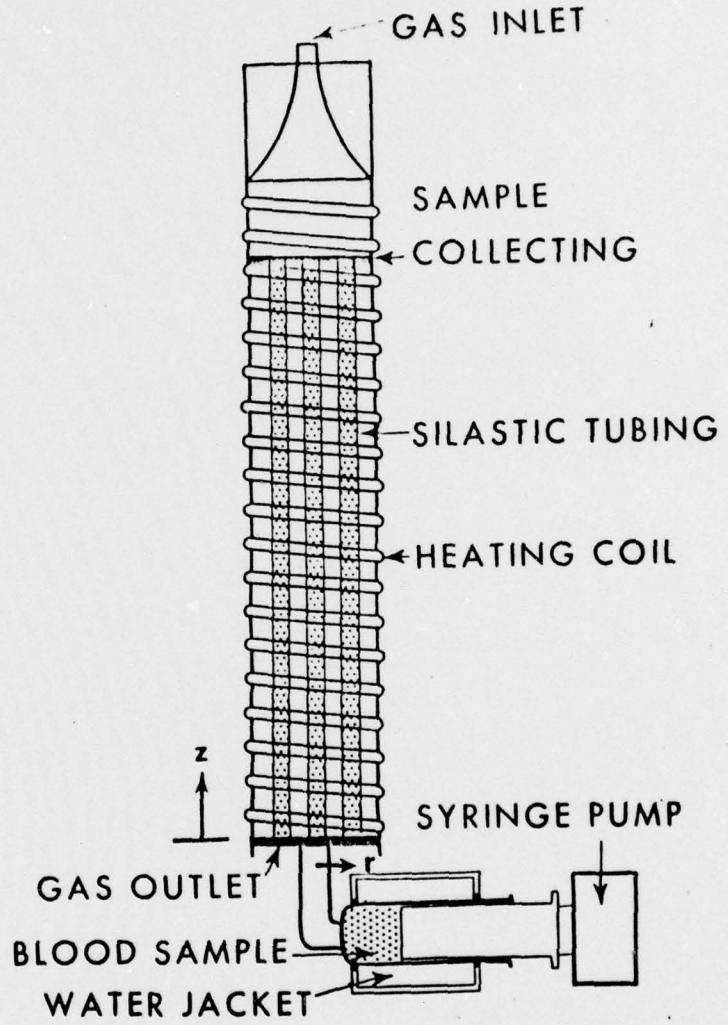


Figure 5

Apparatus for blood-gas exchange

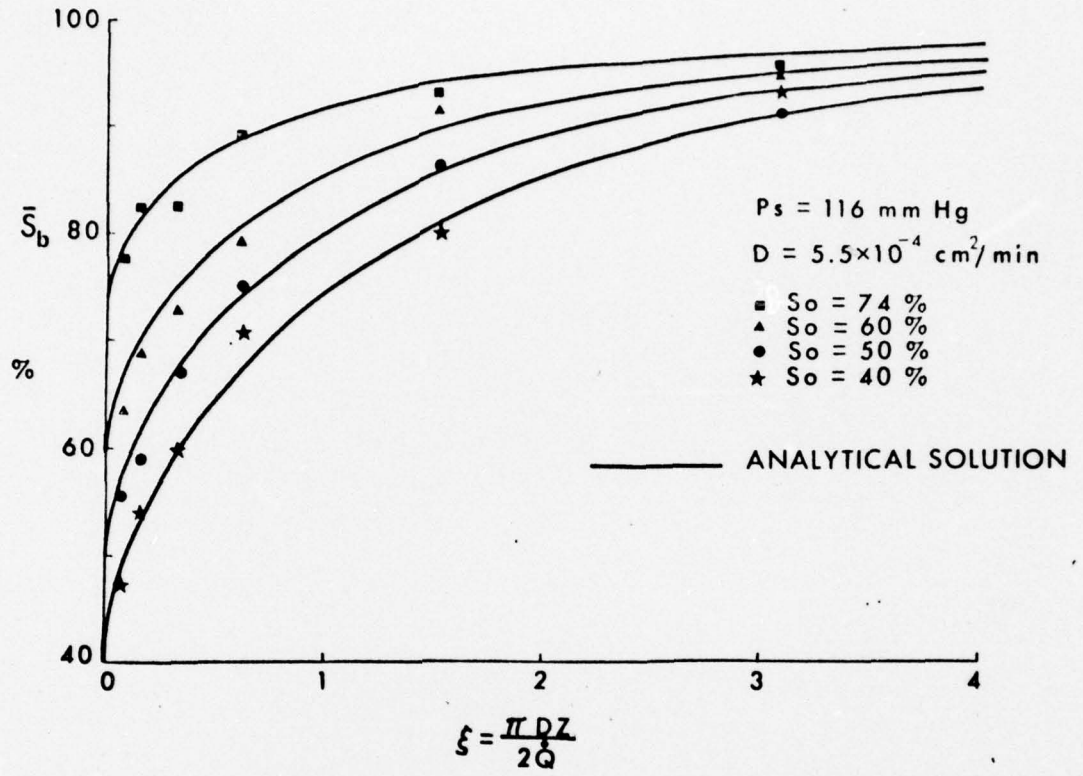


Figure 6

Comparison between experimental data and analytical results at different initial saturations.

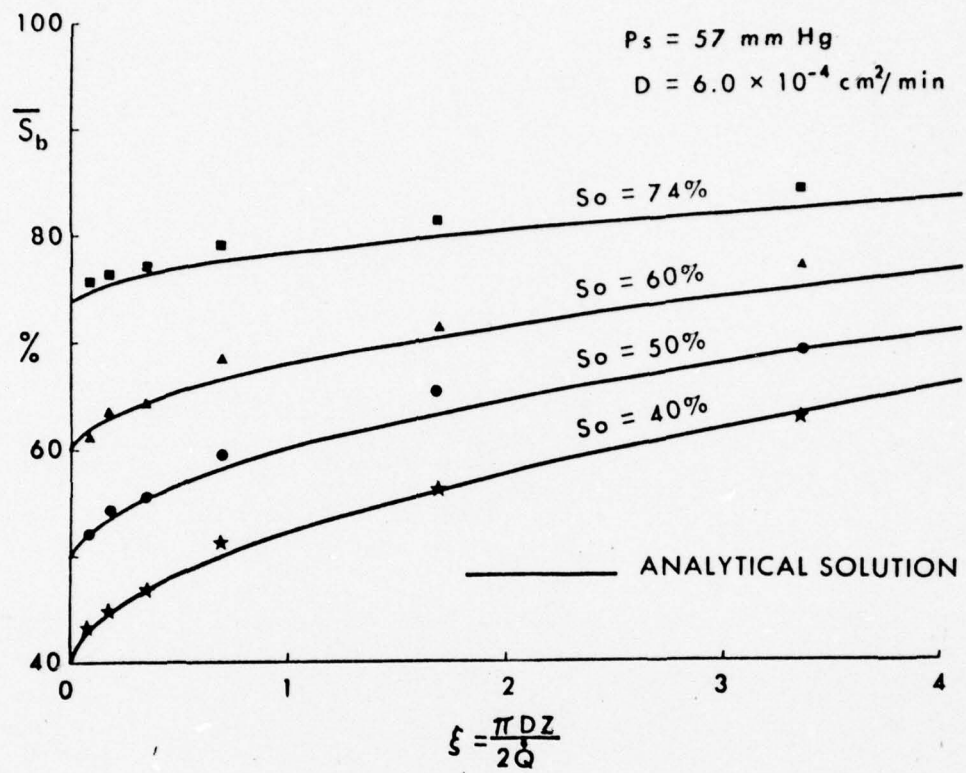


Figure 7

Comparison between experimental data and analytical results at different initial saturations at a lower ambient O_2 level.

shown in these graphs. At two different ambient pressures $P_s = 116$ mm Hg and $P_s = 57$ mm Hg it is found that diffusivity is 5.5×10^{-4} cm²/min respectively. The difference between these values is beyond the range of measurement errors and suggests that O₂ transfer is enhanced at low O₂ levels.

Figure 8 shows that the diffusing capacity is a function of blood flow rate as predicted by equation (16a). The higher value of D_L at lower ambient P_{O_2} and lower initial saturation is probably due to the dependence of D_L on the slope of the dissociation curve, as predicted by equation (16c). Because of the larger value of dS/dC_b^* in the lower part of the dissociation curve there is a strong sink effect associated with the lower value of P_s than with the higher P_s . Experimental results calculated both by the present model analysis as well as by the classical Bohr integration are shown in Figure 8. Close agreement between these two different methods is probably due to the insensitivity of the pressure gradient, $P_s - \bar{P}$ to changes in the value of \bar{P} .

The assumption of negligible wall resistance in the present system is tested by oxygen diffusion in plasma where no sink effect exists. In this case equation (2) is reduced to a linear differential equation and the integral method of solution can again be applied. The minimal dependence of O₂ transport on γ as shown in Figure 9 implies that the present assumption of negligible wall resistance γ is justified. The diffusion of oxygen in blood whose Hb is converted to met Hb is also studied and a substantial decrease of O₂ uptake is observed as compared to the normal blood.

Conclusion: The simplified model for blood oxygenation analysis presented here is qualitatively in agreement with the experimental data. This indicates that the assumptions of a diffusion limited process and parabolic velocity profile are reasonable. Owing to the flattening of the O₂ dissociation curve, the rate at which P_{O_2} increases along the capillary is dependent upon the ambient O₂ level. It is observed that the diffusing capacity is a function of the blood flow rate as well as the sink strength and the initial level of blood oxygenation. Therefore, the shape of the dissociation curve is important in determining the value of D_L .

In the present study the size of the membrane tubing is much greater than the size of a red cell. For future work, in order to simulate pulmonary capillary blood flow, small tubing of physiological capillary diameter is proposed. In that case, the parabolic velocity profile is clearly not valid and modification would have to be made.

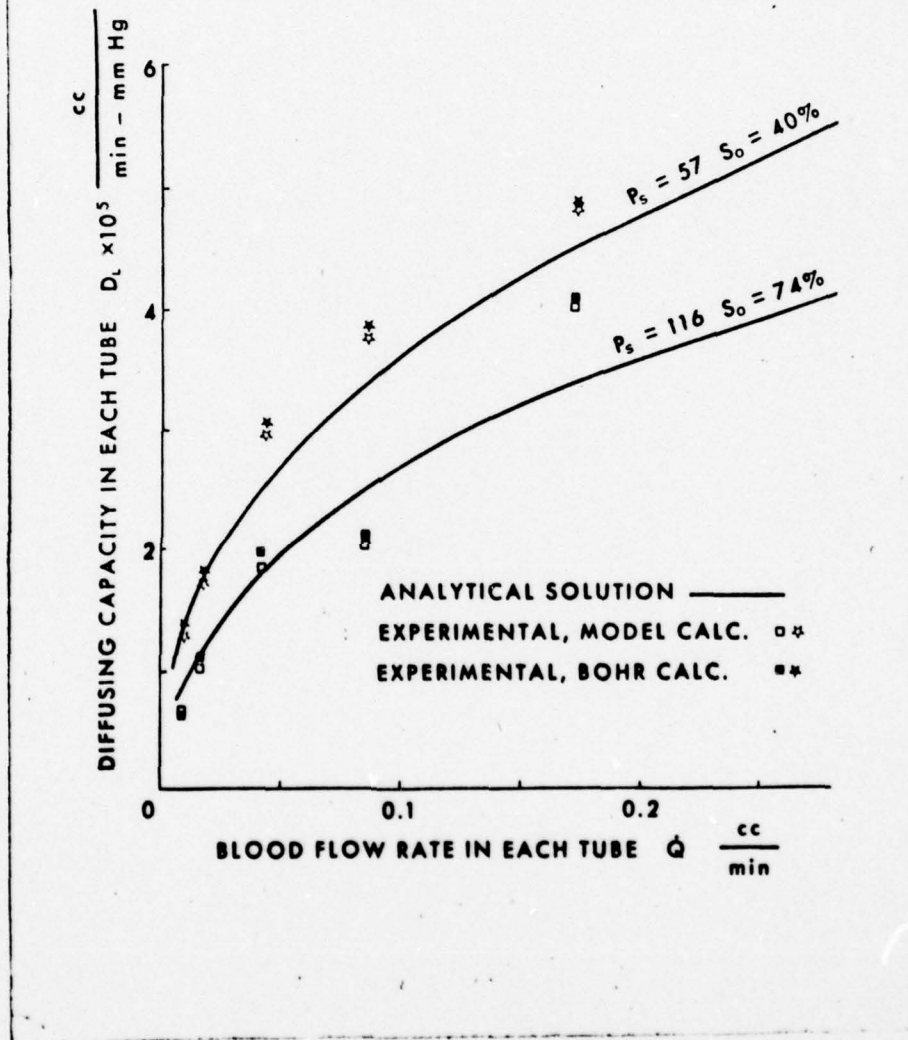


Figure 8

Diffusing capacities versus flow rates at two O_2 levels.

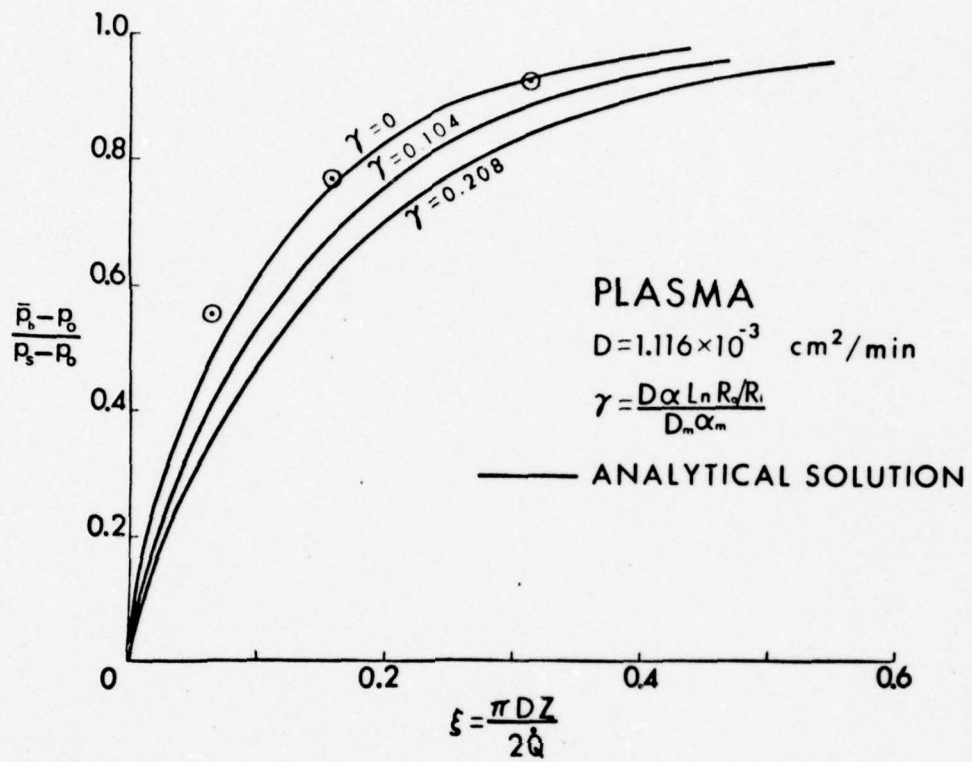


Figure 9

Influence of membrane wall resistance γ on O_2 transfer into plasma. The value of D is obtained from ref. 2.

APPENDIX A

$$H_1(\delta) = \frac{5\delta^6 - 16\delta^5 - 28\delta^4 + 112\delta^3}{140}$$

$$H_2(\delta) = \frac{11\delta^7 - 20\delta^6 - 188\delta^5 + 272\delta^4 + 1176\delta^3}{840(4 + \delta)}$$

$$H_3(\delta) = \frac{265\delta^8 - 24\delta^7 - 7304\delta^6 - 2504\delta^5 + 78624\delta^4 + 126880\delta^3}{40040(4 + \delta)^2}$$

$$H_4(\delta) = \frac{5}{6}\delta^6 - \frac{26}{5}\delta^5 + 11\delta^4 - 40\delta^3 + 704 \left[\frac{1}{2}(\delta + 4)^2 - 8(\delta + 4) \right. \\ \left. + 24 + 16 \ln \frac{\delta + 4}{4} \right]$$

$$H_5(\delta) = \frac{11}{6}\delta^6 - \frac{86}{5}\delta^5 + 71\delta^4 - \frac{1000}{3}\delta^3 + 2588\delta^2 - 23056 \left[\delta - 8 \ln \frac{\delta + 4}{4} \right. \\ \left. - \frac{16}{4 + \delta} + 4 \right] - 82816 \left[\ln \frac{4 + \delta}{4} + \frac{4}{4 + \delta} - 1 \right]$$

$$H_6(\delta) = \frac{265}{6}\delta^6 - \frac{2674\delta^5}{5} + 3004\delta^4 - \frac{49912\delta^3}{3} + 133464\delta^2 - 1292256\delta$$

$$H_7(\delta) = \frac{-767832\delta^2}{(4 + \delta)^2} + 1535664 \ln \frac{4 + \delta}{4} - \frac{5093568}{4 + \delta} + \frac{12134400}{(4 + \delta)^2} + 514992$$

B. Measurement of CO Diffusion Capacity Using a New Steady-State Method

Introduction: Current steady-state methods of measuring pulmonary carbon monoxide diffusing capacity while usually being reasonably accurate and appreciable have several disadvantages. The Filley method requires an arterial blood sample and the Bates and Henderson-Haggard methods require end-tidal sampling. The latter has two disadvantages. In normal people shallow and deep breathing cause falsely low and high estimates of D_{CO} respectively and, in people with abnormal lungs, end-tidal gas composition may not reflect that of mixed alveolar gas. This laboratory has recently developed a steady-state method of CO diffusing capacity measurement that does not require end-tidal sampling.

Theory: Symbols: x, x_1, x_2, x_3 = inspiratory CO, O₂, CO₂, N₂ fraction
 y, y_1, y_2, y_3 = end-tidal CO, O₂, CO₂, N₂ fraction
 z, z_1, z_2, z_3 = mixed expiratory CO, O₂, CO₂, N₂ fraction
 V_D = Dead Space Vol. (BTPS)
 V_T = Tidal Vol. (BTPS)
 f = frequency (min⁻¹)
 D_{LCO} = CO diffusing capacity = $D/0.863$ (ml CO-mm Hg⁻¹
 -min⁻¹)
 $x' = x \cdot z_3/x_3$

From the Bohr relation:

$$y = \frac{V_T z - V_D x}{V_T - V_D} \quad (1)$$

The expression for CO uptake (BTPS) can be written:

$$\dot{V}_{CO} = f V_T (x - y) \quad \text{if } R = 1 \quad (2)$$

and $f V_T (x' - z) \quad \text{if } R \neq 1. \quad (2a)$

Filley et al have shown that (20)

$$D = f V_T \frac{(x - z)}{y} \quad \text{if } R = 1 \quad (3)$$

$$= f V_T \frac{(x' - z)}{y} \quad \text{if } R \neq 1. \quad (3a)$$

Equations (1) and (3) and (1) and (3a) can be combined to give:

$$I = \frac{x}{x - z} = \frac{f V_T}{D} + \frac{V_T}{V_T - V_D} \quad \text{if } R = 1 \quad (4)$$

where $x/(x - z) = I$ or the "impediment" to CO gas transfer from inspired gas to pulmonary blood. This is approximately equal to the reciprocal of the fraction of CO removed from inspired gas.

If $R \neq 1$ the above becomes

$$I' = \frac{x}{x' - z} = \frac{f V_T}{D} + \frac{V_T}{V_T - V_D} \frac{x - z}{x' - z} \quad (4a)$$

If the subject then breathes at a constant tidal volume but at two different frequencies, the resulting simultaneous equations can be subtracted to give:

$$I_1 - I_2 = (f_1 - f_2) \frac{V_T}{D} \quad \text{if } R = 1 \quad (5)$$

with the last term "dropping out".

If $R \neq 1$ and one assumes that

$$\frac{x - z(1)}{x'(1) - z(1)} - \frac{x - z(2)}{x'(2) - z(2)} \approx 0$$

then
$$I_1' - I_2' = \frac{(f_1 - f_2) V_T}{D} .$$

The above expressions can be solved for D easily.

As people exposed to environmental and/or experimental CO build up a significant blood CO concentration which equilibrates with their alveolar gas, the estimation of this CO "back pressure" becomes important.

If "alveolar back pressure" is measured

$$z \text{ "true"} = z \text{ "measured"} - 3/4 y \text{ (back pressure)} \quad (6)$$

(empiric formula)

If "mixed expiratory back pressure" is measured

$$z \text{ "true"} = z \text{ "measured"} - z \text{ (back pressure)} \quad (7)$$

Thus the final formula becomes:

$$D_{LCO} = \frac{V_T (f_1 - f_2)}{0.863 \left[\frac{x}{x'(1) - z \text{ "true"}(1)} - \frac{x}{x'(2) - z \text{ "true"}(2)} \right]}$$

Supine subjects, their tidal volume kept constant by a metering device built into the spirometer, breathe 0.1% CO at a high frequency 18 - 20/min for a 4 min rinse period to achieve a steady state. A 2-minute collection of mixed expiratory and end-tidal gas is then made. After a short interval a similar rinse and collection is made with the subject breathing at a low frequency (6-10/min) but the same tidal volume. All the above collected gas is then analyzed in a gas chromatograph (Beckman GC-5, Beckman Instruments, Fullerton, Calif.). CO back pressure is determined by the rebreathing method before the study, between the two runs, and after the second run to give an estimate of back pressure for each run.

Results: To date three normal subjects have been measured. The precision of the impediment method compares favorably with that of the Bates method.

Subject	<u>DCOBates</u>	<u>% SD</u>	<u># runs</u>	<u>DCOIcorr</u>	<u>% SD</u>	<u># runs</u>
JSK	43.3	9.9	8	39.3	7.5	8
SS	29.8	6.1	9	31.9	8.0	9
ML	27.0 [†]	20.0	9	33.1	27.9	7
	25.4 [‡]	31.3	9	24.0 [#]	32.3	7

*Uncorrected for back pressure $f \approx 9$

†Uncorrected for back pressure $f \approx 19$

#Uncorrected for back pressure

Discussion: The method appears to be theoretically and practically sound, reasonably accurate and precise, and it does not require end-tidal sampling or invasion of the patient.

Its advantages are that this method may, in fact, give the "true D", a factor that may be especially important with people with pulmonary disease whose "true diffusing capacity" may well differ significantly from their measured diffusing capacity. This, however, remains to be measured in such patients.

Its disadvantages are that: 1) it requires two separate steady state runs, one of them at a level of hyperventilation that can be uncomfortable; 2) it requires CO back pressure estimation. Both of the above make the procedure time consuming for patient and technician; 3) it requires a fairly high degree of patient cooperation and therefore might not be applicable for ill subjects; 4) it requires fairly complex equipment i.e. tidal volume regulation; 5) the solution of the equations are laborious and are best done by a computer; and 6) it requires a fairly wide $\Delta f_1 - f_2$; otherwise $\Delta I_1 - I_2$ becomes a small number in which small errors are magnified into large errors in the final D.

C. Effect of Pentobarbital on Ventilatory Drive

Introduction: Although barbiturates are widely used as preoperative sedatives, little is known of their effects on the control of breathing. While it is widely believed that these agents do not depress the ventilatory response to hypoxia (15), good evidence on this point is lacking. In order to resolve this question, we studied the effect of pentobarbital on hypoxic ventilatory drive in normal human subjects.

Methods: Seven males and three females, all in good health between the ages of 24 and 42 years of age, were the subjects. All were born at low altitude and had been residing in Denver, Colorado (elevation 1600 meters) for months to years. All studies were performed in our laboratory in Denver. End-tidal oxygen and carbon dioxide tensions ($P_{A_{O_2}}$ and $P_{A_{CO_2}}$) were continuously monitored. Subjects initially breathed 40% oxygen to which nitrogen was added such that the $P_{A_{O_2}}$ was gradually lowered to 40 torr. Changes in $P_{A_{CO_2}}$ were prevented by the addition of carbon dioxide to the inspired air in

amounts sufficient to prevent the development of hypocapnia. Hypoxic ventilatory drive was evaluated as previously described (see progress report No. IV) and (14) by fitting the $V_E - P_{A}O_2$ data points to the equation:

$$V_E = V_0 + \frac{A}{P_{A}O_2 - 32}$$

where V_E is minute ventilation in liters per minute BTPS and V_0 is the asymptote for ventilation obtained by extrapolation. The parameter A describes the shape of the curve such that the greater the hypoxic drive the higher the A value. Two control hypoxic drive studies were performed on each subject, after which pentobarbital 2 mg/kg was administered intramuscularly. Measurements of hypoxic drive were made 30, 40, 60, 75 and in some cases 105 minutes after injection. Resting ventilation was calculated as V_E at $P_{A}O_2 = 120$ mm Hg from the subjects A value.

Maximal oxygen uptake was measured by a modified Balke test. With the treadmill set at 3.5 mph, the subject walked for 10 minutes at a predetermined grade. Then the treadmill speed was increased to 7 mph and the subject ran at this predetermined grade. Every 2 minutes the treadmill grade was increased 2%. The test continued until the subject signaled his inability to continue. Expired gas was collected in bags during the last 30 seconds of each 2 minute work load and gas samples analyzed by chromatography.

To determine whether hypoxic ventilatory drive was altered in a given subject by pentobarbital, the two control values on each subject were compared to the four values on the same subject under the influence of the drug using an unpaired t-test (10). The significance level was taken as $p < .1$ for separation of the two groups. Maximal oxygen uptake in the two groups was compared using an unpaired t-test (10).

Results: Anthropomorphic data relating to the subjects are shown in Table I. All ten subjects exhibited drowsiness approximately 30 minutes after the pentobarbital injection which gradually dissipated by 105-120 minutes. Minute ventilation and end-tidal carbon dioxide were unaltered by the drug (Table II).

Hypoxic ventilatory drive was depressed by pentobarbital in five subjects (30-50% depression) and unchanged in the other 5 (Table III and Figure 10). Within the group showing depression of hypoxic drive, changes were first observed at 30 minutes and had become maximal by 60 minutes. In all but one subject, hypoxic drive had returned to normal by 120 minutes, as shown in Figure 11.

It appeared that this group of subjects might be comprised of 2 separate subgroups with different responses to pentobarbital. In these 2 subgroups ages were not statistically different nor were weights, resting ventilation, or $P_{A}CO_2$. There were 3 females and 2 males in the depressed group and 5 males in the nondepressed group. Resting heart rates were lower (see Table III) 58 ± 3 as opposed to 71 ± 5 beats per minute ($P < .05$) in the group that showed no change in hypoxic ventilatory drive. In addition, maximal oxygen uptake was higher in this group, (49 ± 2.63 as opposed to 33 ± 2.05) ($p < .001$), (Table IV).

TABLE I. ANTHROPOMORPHIC DATA

	<u>Sex</u>	<u>Age (yrs.)</u>	<u>Ht. (cm)</u>	<u>Wt. (kg)</u>
CAH	F	29	155	53.6
REM	M	31	189	64.7
AT	M	26	174	70.0
ML	F	24	160	54.4
HC	M	37	170	57.1
JSK	M	24	180	58.9
FH	M	28	175	78.0
FIH	M	33	188	97.4
LL	M	41	175	82.5
BK	F	42	165	70.0
Mean		31.5	173.1	68.7
SEM		2.09	3.50	4.45

HYPOXIC DRIVE BEFORE AND DURING PENTOBARBITAL 2/mg/kg

Time After Pentobarbital

Resting Ventilation l/min	0 Minutes			30 Minutes			45 Minutes				
	$P_{A}CO_2$ mm Hg	\dot{V}_O	Λ	Resting Ventilation l/min	$P_{A}CO_2$ mm Hg	\dot{V}_O	Λ	Resting Ventilation l/min	$P_{A}CO_2$ mm Hg	\dot{V}_O	
6.64	30	2.72	345	9.10	31	216	6.65	8.86	31	149	7.17
4.98	35	3.54	135	8.37	35	150	6.67	6.84	36	185	4.74
10.59	36	8.75	162	10.85	36	128	9.40	9.72	36	179	7.69
5.36	37	3.73	143	6.11	39	154	4.36	4.81	39	126	3.38
6.89	40	5.95	83	7.30	40	49	6.75	7.68	40	38	7.25
8.39	33	6.65	153	6.73	32	223	4.20	7.95	32	209	5.57
11.13	35	10.5	55	10.21	35	68	9.44	9.56	35	55	8.93
10.93	34	9.20	152	10.95	33	121	9.57	8.48	34	166	6.59
7.54	36	5.00	224	9.18	33	131	7.69	8.25	33	144	6.61
9.55	34	8.42	99	8.66	36	60	7.88	8.32	35	62	7.62
8.20	35	6.45	155.1	8.75	35	130.8	7.26	8.05	35	131.3	6.53
.72	.72	.85	25.77	.53	.92	18.68	.615	.45	.90	18.92	.50

TABLE II. Cont'd.

60 Minutes				75 Minutes				120 Minutes			
Resting Ventilation l/min	P _A CO ₂ mm Hg	A	V _O	Resting Ventilation l/min	P _A CO ₂ mm Hg	A	V _O	Resting Ventilation l/min	P _A CO ₂ mm Hg	A	V _O
9.26	31	162	7.42	9.85	32	153	8.05	10.33	32	333	6.60
6.74	37	132	5.24	8.00	37	119.	6.65				
7.50	35	141	5.90	10.76	36	119	9.41				
5.71	39	98	4.60	5.72	39	98	4.61	5.95	37	165	4.07
6.79	41	63	6.07	6.75	41	73	5.92	5.99	41	128	4.44
6.65	32	166	4.76	8.04	31	141	6.44				
9.33	34	60	8.65	10.38	35	55	9.75				
13.43	33	143	11.8	9.41	35	144	7.77				
10.83	29	3	10.8	12.20	31	79	11.3	10.21	29	111	8.95
8.33	34	44	7.83	7.44	34	56	6.80	8.16	34	99	7.03
8.46	35	101.2	7.31	8.86	35	104.27	7.67	8.12	35	167.2	6.22
.74	1.16	17.71	.79	.63	1.05	11.86	.63	.98	2.06	42.92	.89

TABLE III. HYPOXIC DRIVE DURING PENTOBARBITAL IN 2 SUBGROUPS:

DEPRESSION

Subject	Resting Heart Rate Beats/min	VO ₂ Max ml/kg/min	Time in min. after Pentobarbital						
			0	30	45	60	75	120	
CAH	80	32.3	358	331	216	149	162	158	333
ML	63	34.6	135	151	154	154	98	98	126
HC	76	37.2	81	85	48	38	63	73	128
LL	80	35.6	199	250	131	144	3	79	111
BK	55	25.5	100	97	69	62	44	56	99
Mean	70.8 [†]	33.4 [†]	178.8		123.6	103.8	74.0	92.8	167.2
SEM	5.03	2.05	48.21		30.18	22.62	26.82	17.63	42.9

P<.05[†] P<.01[†]

NON DEPRESSION

Subject	Resting Heart Rate Beats/min	VO ₂ Max ml/kg/min	Hypoxic Ventilatory Drive (A) OS Time in min. after Pentobarbital					
			0	30	45	60	75	
REM	52	55.0	149	121	150	185	132	119
AT	52	48.8	157	166	128	179	141	119
SK	54	54.0	175	130	223	209	166	151
FHu	68	40.3	53	56	68	55	60	55
FHei	63	47.6	166	133	121	166	143	144
Mean	57.8 [†]	49.1 [†]	131.4		138.0	158.8	128.4	115.6
SEM	3.26	2.63	19.59		25.16	26.87	18.00	16.04

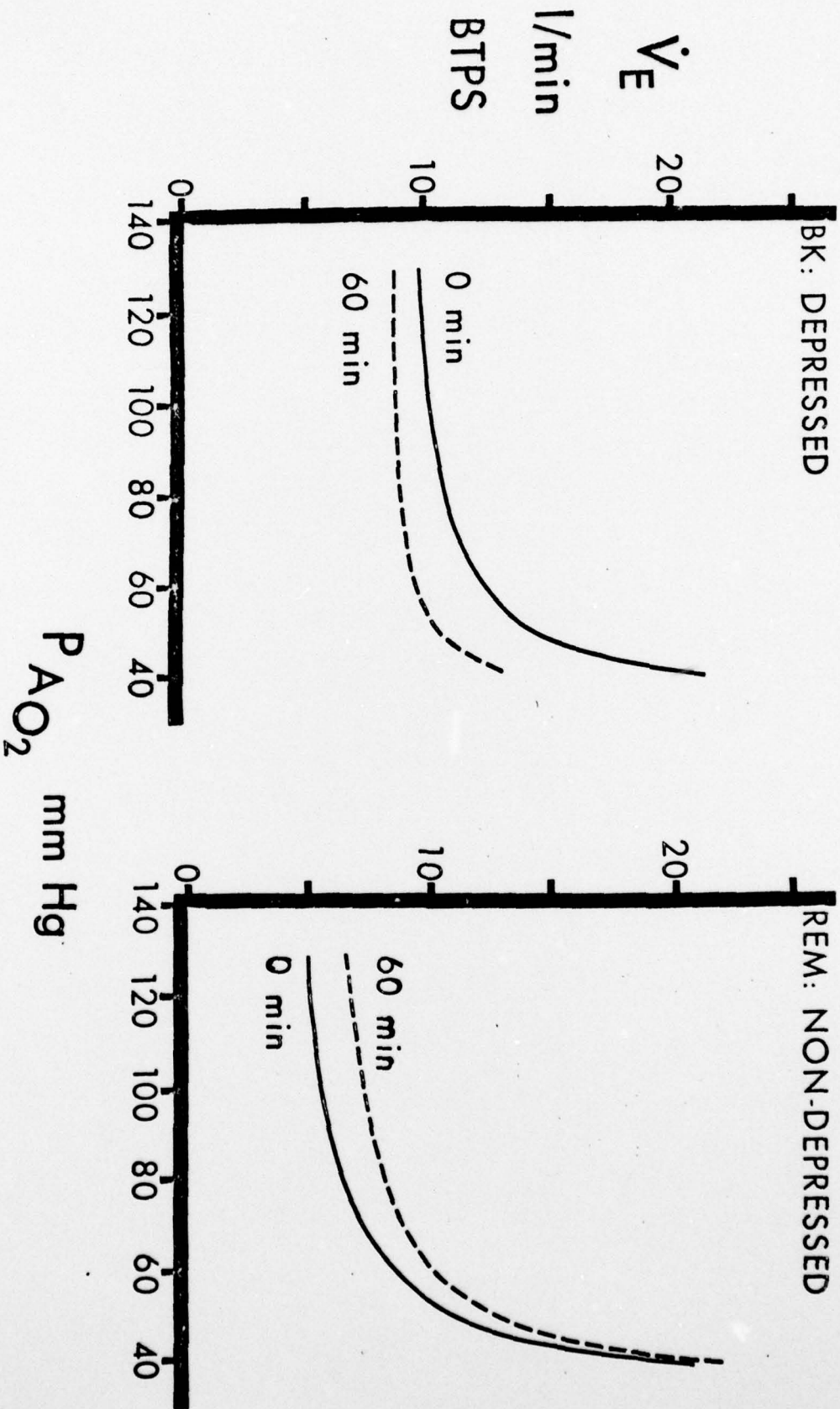
Paired T test was used to compare 2 control A values with 4 A values after Pentobarbital

TABLE IV

Maximum O ₂ Uptake		ml/kg/min	
Depressed Group		Non-Depressed Group	
Subject	VO ₂ max.	Subject	VO ₂ max.
SK	54.0	CAH	32.3
REM	55.0	ML	34.6
AT	48.8	HC	37.2
F Hei	47.6	BK	25.5
F Hu	40.3	LL	35.6
\bar{x}	49.1 ± 2.63	\bar{x}	33.4 ± 2.05

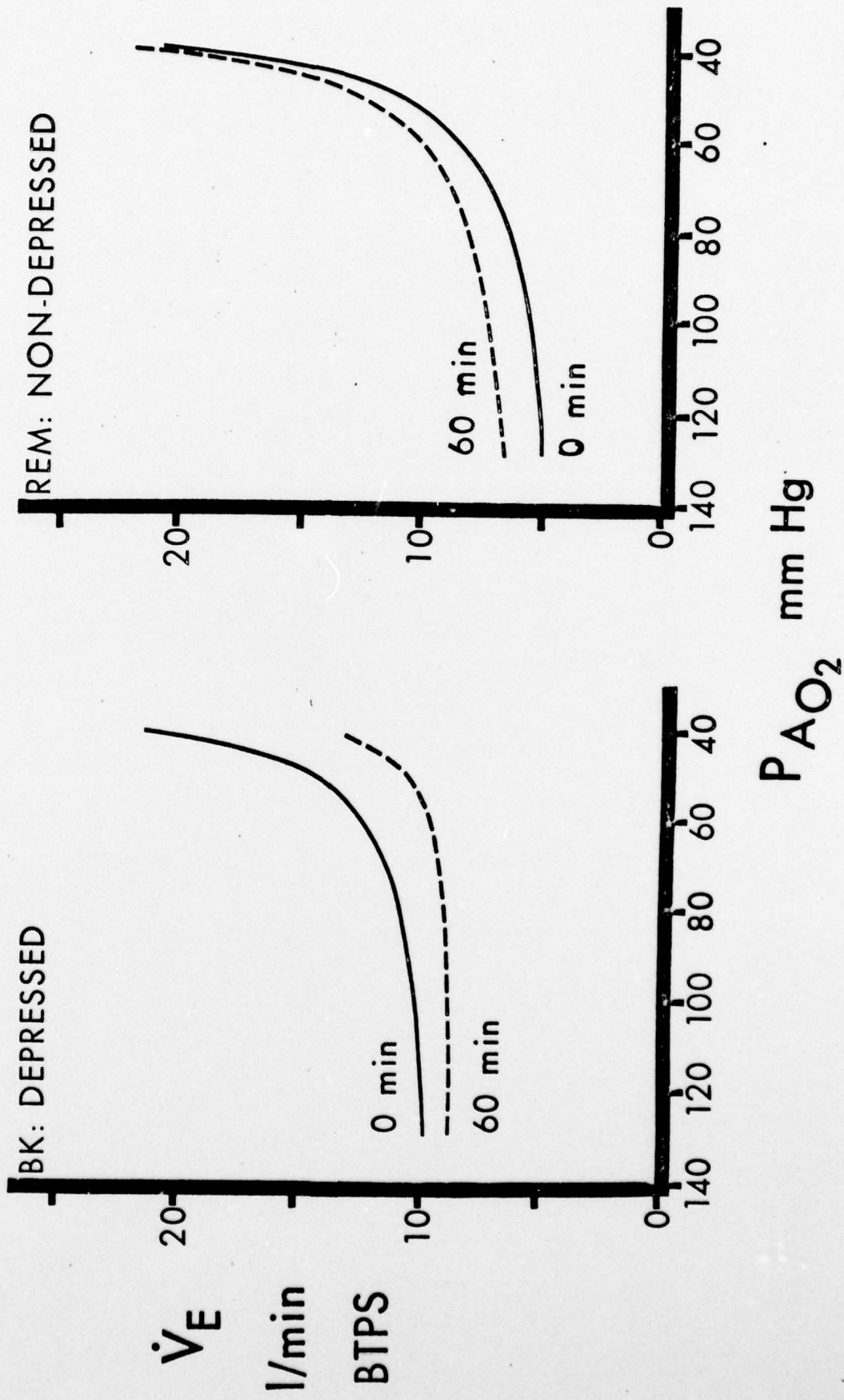
p < .001

EFFECT OF PENTOBARBITAL ON HYPOXIC VENTILATORY DRIVE



subject to the left and no change in the subject on the right.

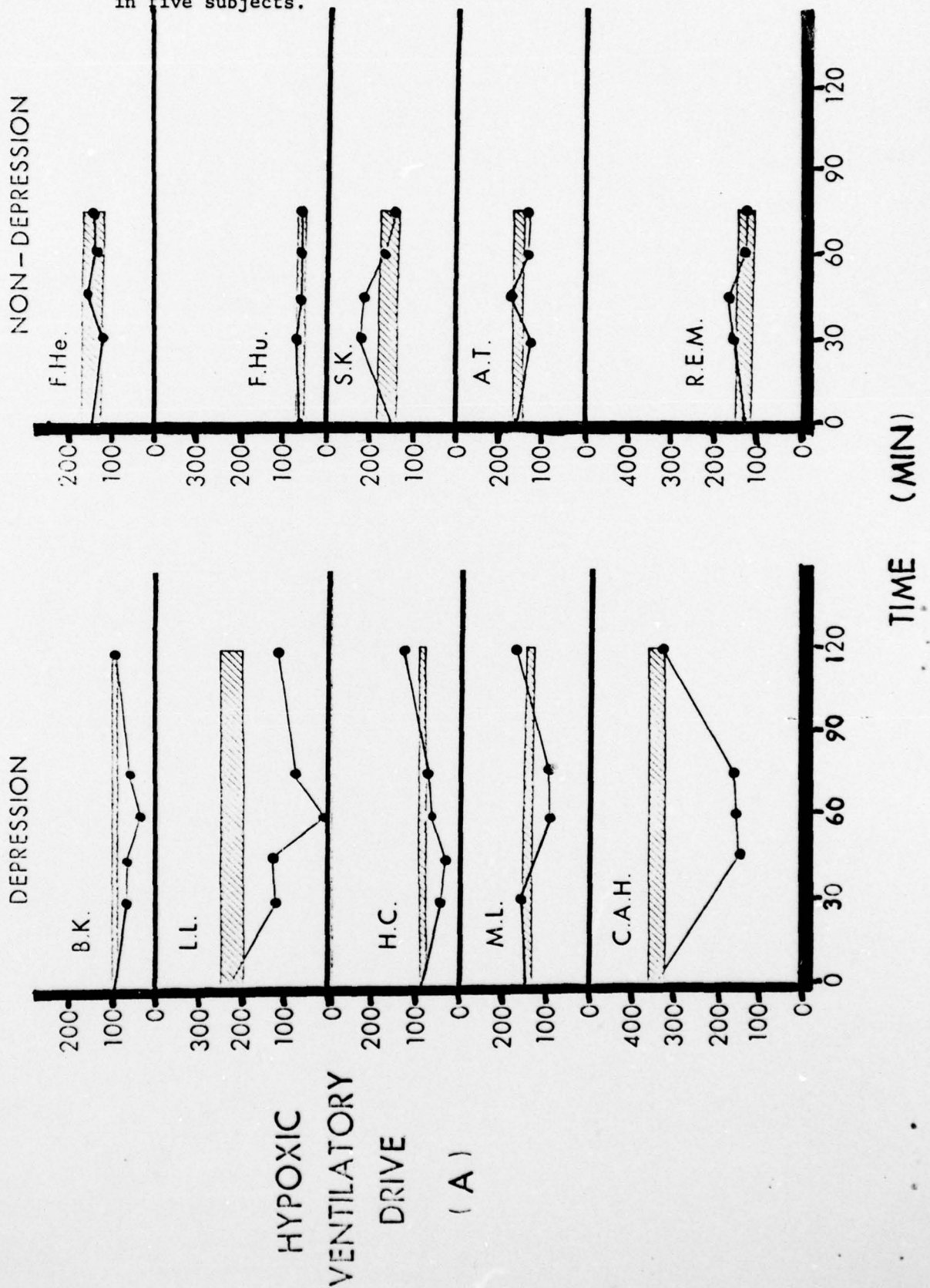
EFFECT OF PENTOBARBITAL ON HYPOXIC VENTILATORY DRIVE



subject to the left and no change in the subject on the right.

HYPOXIC VENTILATORY DRIVE DURING PENTOBARBITAL

Figure 11: The "hatched" area represents the two control hypoxic ventilatory drive values. The results indicate a marked blunting of hypoxic drive in five subjects (30 to 50%) and no change in hypoxic drive in five subjects.



Discussion: In healthy subjects pentobarbital in amounts commonly used to produce mild sedation has no effect on resting ventilation or resting $P_{A}CO_2$ but did depress hypoxic ventilatory drive in half the subjects. Absence of alterations in resting ventilation is in agreement with Stephen et al (13) who found no hypoventilation with a comparable dose of secobarbital. Keats et al (12) found an increase in ventilation after 1.4 mg/kg pentobarbital but a decrease after 2.8 mg/kg. The most clear-cut evidence of a respiratory effect of pentobarbital was a depression of hypoxic drive in five of our subjects and no change in hypoxic drive in the remaining five. Little has been written regarding the effects of barbiturates on hypoxic ventilatory drive. In fact, the only previous study found (11) demonstrated in one subject that triple conventional doses of cyclobarbitol resulted in some depression of ventilation during hypoxia. However, only very mild hypoxia was employed ($P_{A}O_2 = 60$ mm Hg), which is insufficient to produce a well developed hypoxic response in normal man (14).

In half the subjects, there was no depression of hypoxic ventilatory drive with pentobarbital. There appeared to be two populations represented in our sample which differ with respect to the suppressibility of their hypoxic drive with pentobarbital. These subgroups also differ in their physical condition as measured by maximal oxygen uptake and resting heart rate. Subjects whose ventilatory drive was unaffected by pentobarbital and who were all involved in athletic activities on a regular basis had lower resting heart rates and higher maximal oxygen uptake than the subjects in the group that showed depression of hypoxic drive. Byrne-Quinn et al (9) found that hypoxic drive was lower in true athletes at rest than in nonathletes. While we found no significant differences in control levels of hypoxic ventilatory drive between the two groups, some other factor distinguishing athletes from nonathletes could account for the differences in response to the drug. Body weight was similar in the two groups and moreover the drug was administered on a weight basis.

However, it is possible that differences in lean body mass or in drug metabolism or redistribution could account for this difference. Unfortunately, we do not have barbiturate blood levels on any of our subjects and cannot exclude the possibility that differences in drug metabolism may have contributed to the different effects in the two groups. This study was not carried out with a double blind design because we believed that our subjects would all have been able to readily distinguish the difference between pentobarbital and placebo.

This study suggests that sedentary, less physically fit individuals are more likely to exhibit depression of hypoxic ventilatory drive where pentobarbital is administered.

D. References

1. Bartlett RH, Noyes BS Jr., and Drinker PA: A simple reliable membrane oxygenator for organ perfusion. J. Appl. Physiol. 29:758-759, 1970.
2. Briehl RW, and Fishman AP: Principles of the Bohr integration procedure and their application to measurement of diffusing capacity of the lung for oxygen. J. Appl. Physiol. 15:337-348, 1960.
3. Buckles RG, Merrill EW, and Gilliland ER: an analysis of oxygen absorption in a tubular membrane oxygenator. AIChE. J. 14:703-708, 1968.
4. Goodman RT: The heat balance integral and its application to problems involving a change of phase. Trans. ASME 80:335-346, 1958.
5. Hershey D: Blood Oxygenation. New York, Plenum Publication Corp., 1970.
6. Schlichting H: Boundary Layer Theory. English Translation by J. Kestin. New York, McGraw Hill Book Co., Inc., 1960.
7. Weissman MH, and Mockros LF: Oxygen transfer to blood flowing in round tubes. J. Engng. Mech. Div. Am. Soc. Civ. Engrs. 98:225-245, 1967.
8. Weissman MH, and Mockros LF: Oxygen and carbon dioxide transfer in membrane oxygenators. Med. and Biol. Engng. 7:169-184, 1969.
9. Byrne-Quinn E, Weil JV, Sodal IE, Filley GF, and Grover RF: Ventilatory control in the athlete. J. Appl. Physiol. 30:91-98, 1971.
10. Dixon WJ, and Massey FG: Introduction to Statistical Analysis. Third Edition, New York, McGraw Hill 1969, p. 109.
11. Harris EA, and Dawson KB: The respiratory effects of therapeutic doses of cyclobarbitone, triclofos and ethchlorvinol. Brit. J. Pharmacol. 24:214-222, 1965.
12. Keats AS, Jorosu Y: Increased ventilation after pentobarbital in man. Fed. Proc. 16:311, 1957.
13. Stephen GW, Banner MP, Wollman H, Smith TC: Respiratory pharmacology of mixtures of Scopolomine with Secobarbital and with Fentanyl. Anesthesiology 31:237-242, 1970.
14. Weil JV, Byrne-Quinn E, Sodal IE, Friesen WO, Underhill B, Filley GF, and Grover RF: Hypoxic ventilatory drive in normal man. J. Clin. Invest. 49:1061-1071, 1970.
15. Wylie WD, and Churchill-Davidson HC: A Practice of Anaesthesia, Third Edition, Year Book Medical Publishers, Chicago, 1972, p. 92.
16. Branscomb BV, and Wright GW: Effects of controlled low oxygen breathing upon exchange of respiratory gases in humans. Federation Proc. 11:16, 1952.

17. Hill JR: The oxygen consumption of new born and adult mammals. Its dependence on the oxygen tension in the inspired air and on the environmental temperature. J. Physiol. (London) 149:346-373, 1959.
18. Moore RE: Oxygen consumption and body temperature in newborns subjected to hypoxic and reoxygenation. J. Physiol. (London) 149 500-518, 1959.
19. Alpert NR, Kayne H, and Haslett W: Relationship among recovery oxygen, oxygen missed, lactate production and lactate removal during and following severe hypoxia in anesthetized dogs. Am. J. Physiol. 192:585-591, 1958.
20. Filley GF, Bigelow DB, Olson DE, and Lacquet LM: Pulmonary gas transport. A mathematical model of the lung. Am. Rev. Resp. Dis. 98:480-489, 1968.